

Phytohormonal and metabolism analysis of *Brassica rapa* L. ssp. *pekinensis* with different resistance during *Plasmodiophora brassicae* infection

MEI LAN[#]; JINGFENG HU[#]; HONGLI YANG; LIQIN ZHANG; XUEZHONG XU; JIANGMING HE*

Institute of Horticultural Crops, Yunnan Academy of Agricultural Sciences, Yunnan Branch of the National Vegetable Improvement Center, Kunming, 650205, China

Key words: Auxins, Brassicaceae, Clubroot, Cytokinins, Fatty acids, Glucosinolates, Glutathione, Salicylic acid, Jasmonic acid

Abstract: Clubroot of Chinese cabbage (*Brassica rapa* L. ssp. *pekinensis*), caused by the obligate parasite *Plasmodiophora brassicae*, accounts for serious yield losses. The aim of our study was to explore the phytohormone levels and metabolome changes in the roots of resistant and susceptible *B. rapa* genotypes at a late stage of infection, i.e., 28 days post-infection. Both genotypes showed decreased auxin levels after *P. brassicae* infection except for indole-3-acetic acid. Overall, the susceptible genotype had higher auxin and cytokinin levels after infection, with the exception of trans-zeatin and 3-indolebutyric acid as compared to the resistant genotype. Jasmonic acid levels declined after infection regardless of the genotype. Resistance against clubroot was evident with the increased levels of salicylic acid in the resistant genotype. The susceptible genotype had a higher number of differentially accumulated metabolites (DAMs) (262) than the resistant genotype (238) after infection. Interestingly, 132 DAMs were commonly detected in both genotypes when infected with the pathogen, belonging to metabolite classes such as phenolic acids, amino acids, and derivatives, glucosinolates, organic acids, flavonoids, nucleotides and derivatives, and fatty acids. The differential metabolite analysis revealed that metabolites related to amino acid biosynthesis, fatty acid biosynthesis and elongation, glutathione metabolism, and glucosinolate metabolism were highly accumulated in the resistant genotype, suggesting their essential roles in resistance against *P. brassicae* infection.

Introduction

Chinese cabbage (*Brassica rapa* L. ssp. *pekinensis*) is an important economical and nutritious vegetable crop in China (Huang *et al.*, 2017). However, its yield is severely reduced by a soil-borne obligate pathogen: *Plasmodiophora brassicae* (Kayum *et al.*, 2017). *P. brassicae* causes clubroot disease and leads to serious reductions in quality and yield in the members of the family Brassicaceae (Dixon, 2009; Ning *et al.*, 2019). In recent years, the incidence of clubroot has gradually become more serious in China, although it is more severe in the southwest, northeast, and central regions of China (Zhu *et al.*, 2019). Overall, the disease affects 3.2–4.0 million hectares of Brassica crops annually. Due to its pathology and soil-borne nature, it is difficult to control. Furthermore, several environmental factors such as climate,

soil types, humidity, rainfall, and temperature, are known to contribute to the spread of clubroot disease (Chai *et al.*, 2014). Therefore, a complete understanding of the defense mechanisms in host plants against *P. brassicae* is critical for efficient disease management.

Clubroot infection by *P. brassicae* completes in three stages, i.e., an early stage before symptoms appear, the onset of gall formation, and late stages of infection when spores are formed (Ludwig-Müller and Schuller, 2007). Detailed investigations have already established the role of different signaling and resistance pathways during the infection cycles. For example, studies focusing on the early infection stage have demonstrated that a more intense defensive response is produced by resistant lines where plant hormone signal transduction, fatty acid metabolism, and glucoside biosynthesis metabolism pathways regulate the resistance against clubroot (Li *et al.*, 2020). In the second stage, i.e., gall formation, *P. brassicae* infection disrupts mechanisms that regulate the mitotic status of host cells, cell proliferation within galls is reduced as the results of transcriptional reprogramming, and host endoreduplication

*Address correspondence to: Jiangming He, hejiangming666@126.com

[#]Co-first authors

Received: 19 July 2020; Accepted: 23 September 2020



facilitates hypertrophied cell formation (Olszak *et al.*, 2019). During this stage, the gall constitutes a strong metabolic sink for carbohydrate, polyamines, amino acid, proline, and secondary metabolites such as phytoalexins, phytoanticipins, camalexin, indole glucosinolate, and flavonoids. Cell wall compounds, lipids, shikimate pathway metabolites, jasmonic acid biosynthesis genes, cell wall modification, biosynthesis of starch, and transcripts associated with phytohormones are regulated in the hosts during this stage (Irani *et al.*, 2018). However, limited studies have focused on alterations of these pathways at the late stage of spore formation. A recent study investigated the changes in metabolites status in plant–pathogen interaction of clubroot and *Arabidopsis* and reported that the expression of genes associated with amino acid biosynthesis was altered throughout the infection stages, i.e., from early to late stages (Yahaya *et al.*, 2017). However, a complete picture of metabolic changes at the late stages of infection is not available.

The role of phytohormones in *P. brassicae*–plant interaction is a widely investigated topic. Different studies focused on exploring the roles of hormonal pools during clubroot disease development. For example, gall formation stimulates cell division, which requires growth-promoting hormones, i.e., cytokinins and auxins (Ludwig-Müller and Schuller, 2007). Auxin levels have been studied in infected roots during different clubroot infection stages (Devos *et al.*, 2005), which revealed that the level of auxins is non-synchronized (Ludwig-Müller *et al.*, 2009). Therefore, understanding the role of auxins at a particular stage is critical (Kavanagh and Williams, 1981). In contrast to auxins, the role of cytokinins is well established and is consistent. Cytokinin depleted plants have shown better tolerance to clubroot disease (Malinowski *et al.*, 2016). A study examined the *Arabidopsis* root transcriptome in response to clubroot infection and found that the host cytokinin metabolism was strongly downregulated at two states, i.e., onset and late gall formation stages. Furthermore, gene expression and micro-analytical results confirmed the repression of cytokinin biosynthesis, signaling, and degradation, as well as conjugation, were repressed (Siemens *et al.*, 2006). However, it is known that different species within Brassicaceae may adapt different strategies towards clubroot infection (Kobelt *et al.*, 2000). Therefore, understanding the role of these hormones at different infection stages in *B. rapa* can increase our knowledge about defense responses within this species. Clubroot infection not only imposes alterations in growth-promoting hormones but also impacts the signaling and production of stress-responsive and defense-related hormones. Reports on the role of salicylic acid (SA), and jasmonic acid (JA) during early disease infection stages have significantly enhanced our understanding that both JA and SA pathways contribute to basal and partial resistance to the biotrophic clubroot pathogen (Prerostova *et al.*, 2018). However, a complete understanding of the role of these hormones in *B. rapa* at the late stages of infection is missing.

Considering the limited knowledge on the metabolic and phytohormonal changes at the late stages of clubroot disease in *B. rapa*, we have compared the root phytohormones levels and metabolomic profiles of susceptible and resistant

B. rapa genotypes at a late stage of infection, i.e., 28 days post-infection with *P. brassicae*. Our results confirm previously established roles of phytohormones in the early stages of clubroot in *B. rapa* and provide new insights into the root phytohormonal and metabolomic responses at a late stage of infection.

Materials and Methods

Plant material and pathogen inoculation

In this study, we used two *Brassica rapa* L. ssp. *pekinensis* accessions, i.e., a resistant (CCR) and a susceptible (CM), that were obtained from the Cruciferous Subject Group at the Institute of Horticultural Research at the Yunnan Academy of Agricultural Sciences (Lan *et al.*, 2019). Seeds were sown into a 50-cell seedling tray containing a 1:1 mixture of soil and vermiculite. Seedlings were germinated in a phytotron at 25°C for six days until two true leaves were formed. The *P. brassicae* Woronin isolate (Williams, 1966) was collected from a research field at Songming County, Kunming City, Yunnan Province, China. A resting spore suspension (0.5 mL of 1×10^7 resting spores/mL) was added to the surface of the soil around each plant. Control plants, inoculated with 0.5 mL of distilled water, were grown in separate trays in the same phytotron. Plants were treated in blocks, sampled randomly, and the experiment was replicated thrice. Ten individual plants from each repeat were harvested after 14, 21, 28, 35, 42 days post-infection. Root samples were collected, washed thrice with ultrapure double-distilled water, and immediately frozen in liquid nitrogen for biochemical analyses. Root and above ground fresh weights were measured using a weighing balance. Root length was measured using a cm scale.

Phytohormone quantification

Chemicals and reagents

High-performance liquid chromatography (HPLC)-grade acetonitrile (ACN) and methanol (MeOH) were purchased from Merck (Darmstadt, Germany). MilliQ water (Millipore, Bradford, USA) was used in all experiments. All the standards were purchased from Olchemim Ltd. (Olomouc, Czech Republic) and Sigma (St. Louis, MO, USA). Acetic acid was bought from Sinopharm Chemical Reagent (Shanghai, China). The stock solutions of standards were prepared at the concentration of 1 mg/mL in MeOH. All stock solutions were stored at –20°C. The stock solutions were diluted with MeOH to working solutions before analysis.

Sample preparation and extraction

Plant roots (50 g fresh weight) were frozen in liquid nitrogen, ground into powder, and extracted with methanol/water/formic acid (15:4:1, V/V/V). The combined extracts were evaporated to dryness under nitrogen gas stream, reconstituted in 80% methanol (V/V), and filtrated (PTFE, 0.22 µm; Anpel) before liquid chromatography-mass spectrometry (LC-MS/MS) analysis.

HPLC conditions and ESI Q TRAP-MS/MS

The sample extracts were analyzed using an LC-ESI-MS/MS system (HPLC, Shim-pack UFLC SHIMADZU CBM30A

system, www.shimadzu.com.cn/; MS, Applied Biosystems 6500 Triple Quadrupole, www.appliedbiosystems.com.cn/). The analytical conditions were as follows, HPLC: column, Waters ACQUITY UPLC HSS T3 C18 (1.8 μ m, 2.1 mm \times 100 mm); solvent system, water (0.05% acetic acid): ACN (0.05% acetic acid); gradient program, 95:5 V/V at 0 min, 95:5 V/V at 1 min, 5:95 V/V at 8 min, 5:95 V/V at 9 min, 95:5 V/V at 9.1 min, 95: 5 V/V at 12 min; flow rate, 0.35 mL/min; temperature, 40°C; injection volume: 2 μ L. The effluent was alternatively connected to an ESI-triple quadrupole-linear ion trap (Q TRAP)-MS.

AB 6500 Q TRAP LC/MS/MS System, equipped with an ESI Turbo Ion-Spray interface, operating in both positive and negative ion modes and controlled by Analyst 1.6 software (AB Sciex). The ESI source operation parameters were as follows: ion source, turbo spray; source temperature 500°C; ion spray voltage (IS) 4500 V; curtain gas (CUR) were set at 35.0 psi; the collision gas (CAD) was medium. DP and CE for individual MRM transitions were done with further DP and CE optimization. A specific set of MRM transitions were monitored for each period according to the plant hormones eluted within this period.

Phytohormones' contents were detected by MetWare (<http://www.metware.cn/>) based on the AB Sciex Q TRAP 6500 LC-MS/MS platform. Three replicates of each assay were performed (Cui *et al.*, 2015; Xiao *et al.*, 2018).

Metabolite profiling

Sample preparation and extraction

The freeze-dried roots were crushed using a mixer mill (MM 400, Retsch) with a zirconia bead for 1.5 min at 30 Hz. 100 mg powder was weighted and extracted overnight at 4°C with 0.6 mL 70% aqueous MeOH. Following centrifugation at 10,000 g for 10 min, the extracts were absorbed (CNWBOND Carbon-GCB SPE Cartridge, 250 mg, 3 mL; ANPEL, Shanghai, China, www.anpel.com.cn/cnw) and filtrated (SCAA-104, 0.22 μ m pore size; ANPEL, Shanghai, China, <http://www.anpel.com.cn/>) before UPLC-MS/MS analysis.

UPLC Conditions

The sample extracts were analyzed using a UPLC-ESI-MS/MS system (UPLC, Shim-pack UFLC SHIMADZU CBM30A system, www.shimadzu.com.cn/; MS, Applied Biosystems 4500 Q TRAP, www.appliedbiosystems.com.cn/). The analytical conditions were as follows, UPLC: column, Waters ACQUITY UPLC HSS T3 C18 (1.8 μ m, 2.1 mm \times 100 mm); the mobile phase consisted of solvent A, pure water with 0.04% acetic acid, and solvent B, ACN with 0.04% acetic acid. Sample measurements were performed with a gradient program that employed the starting conditions of 95% A and 5% B. Within 10 min, a linear gradient to 5% A and 95% B was programmed, and a composition of 5% A and 95% B was kept for 1 min. Subsequently, a composition of 95% A and 5.0% B was adjusted within 0.10 min and kept for 2.9 min. The column oven was set to 40°C; the injection volume was 4 μ L. The effluent was alternatively connected to an ESI-triple QTRAP-MS.

LIT and triple quadrupole (QQQ) scans were acquired on a triple Q TRAP, API 4500 Q TRAP UPLC/MS/MS

System, equipped with an ESI Turbo Ion-Spray interface, operating in positive and negative ion mode and controlled by Analyst 1.6.3 software (AB Sciex). The ESI source operation parameters were as follows: ion source, turbo spray; source temperature 550°C; IS 5500 V (positive ion mode)/ -4500 V (negative ion mode); ion source gas I (GSI), gas II GSII), CUR were set at 50, 60, and 30.0 psi, respectively; the CAD was high. Instrument tuning and mass calibration were performed with 10 and 100 μ mol/L polypropylene glycol solutions in QQQ and LIT modes, respectively. QQQ scans were acquired as MRM experiments with collision gas (nitrogen) set to 5 psi. DP and CE for individual MRM transitions were done with further DP and CE optimization. A specific set of MRM transitions were monitored for each period according to the metabolites eluted within this period.

Data analysis

Unsupervised principal component analysis (PCA) was performed by statistics function `prcomp` within R (www.r-project.org). The data was unit variance scaled before unsupervised PCA. Significantly regulated metabolites between groups were determined by $VIP \geq 1$ and absolute Log_2FC (fold change) ≥ 1 . VIP values were extracted from Orthogonal Projections to Latent Structures Discriminant Analysis (OPLS-DA) results, which also contain score plots and permutation plots generated using R package `MetaboAnalystR` (Chong and Xia, 2018). The data was log_2 transformed and mean centered before OPLS-DA. In order to avoid overfitting, a permutation test (200 permutations) was performed.

Results

Morphological response of *B. rapa* genotypes against *P. brassicae* infection

Root length of the resistant genotype-CCR followed an increasing trend in infected and control samples, where infected samples had relatively reduced lengths. However, in the susceptible genotype-CM, the root length on 14- and 21-days post-infection (DPI) increased, but from 28 DPI, a significant decrease was noticed as compared to the control (Fig. 1A). The fresh weight of both genotypes showed an increasing pattern with dpi. It is to be noted that the root fresh weight of CM was higher than CCR due to swollen roots (Fig. 1B). The aboveground fresh weight of the resistant genotype increased linearly with the time. However, the infected roots showed reduced above ground weight as compared to controls. Contrarily, in CM, the above ground fresh weight increased on 14 and 21 DPI, but from 28 DPI, it started to decline (Figs. 1C and 1D). These observations suggest that 28 DPI is an important time point in *P. brassicae* infection. In previous investigations, 28 DPI was also reported to be the time point when galls are clearly visible, and cell division, as well as cell elongation, occurs in infected roots (Siemens *et al.*, 2006). Therefore, we focused on exploring the phytohormonal and metabolomics responses of both genotypes against *P. brassicae* infection at this stage.

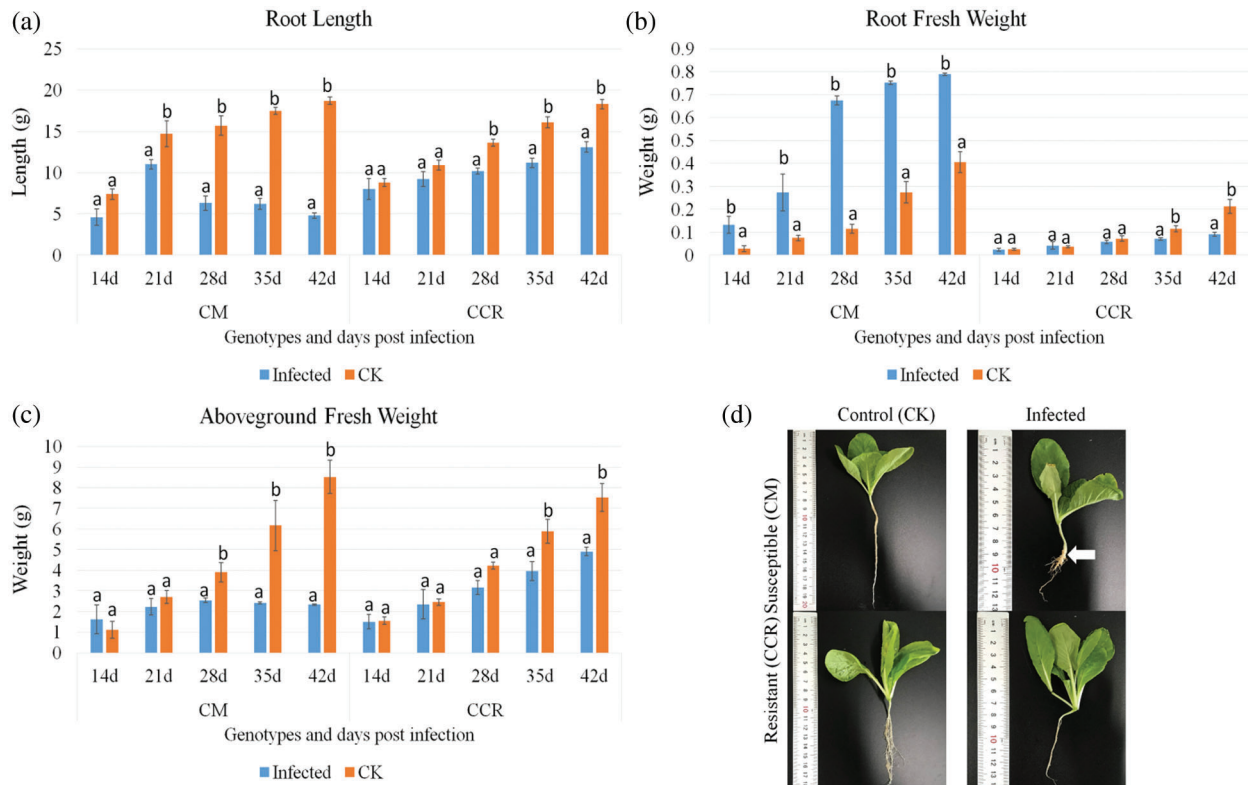


FIGURE 1. Root morphological observations in *B. rapa* infected by *P. brassicae*.

(a) 1-root length, (b) 2-root fresh weight, (c) 3-above ground fresh weight, and (d) 4-phenotype of *B. rapa*. White arrow shows swelling due to the formation of visible galls at 28 days (d) post-infection in susceptible (CM) genotype, while no symptoms are visible in resistant (CCR) genotype. CK = control. Different letters (a, b) on the bars indicate significantly different values.

Phytohormonal responses of *B. rapa* against *P. brassicae* infection

Studies on *Arabidopsis* and *B. rapa* have shown the involvement of phytohormones and related pathways in response to *P. brassicae* infection, mainly at the early stages of infection (Fu et al., 2019; Irani et al., 2018; Siemens et al., 2006). Herein, we studied the phytohormone levels at the late stage of infection between resistant (CCR) and susceptible (CM) *B. rapa* genotypes in order to further understand the contributions of phytohormones in response to the pathogen.

The level of auxins in CM and CCR varied considerably. The content of indole-3-acetic acid (IAA) increased in the CM, while the levels of all other auxins, i.e., methyl indole-3-acetate (ME-IAA), 3-indolebutyric acid (IBA), indole-3-carboxylic acid (ICA), and indole-3-carboxaldehyde (ICAId) decreased in CM's infected samples as compared to control. For the resistant genotype-CCR, the levels of all auxins decreased in infected samples as compared to control. CM had relatively higher IAA, ME-IAA, ICA, and ICAId contents after infection as compared to the CCR, while the level of IBA was higher in CCR as compared to CM (Fig. 2). The level of N6-Isopentenyladenine (IP), which is a naturally occurring cytokinin, decreased in CM after the infection, while in the case of CCR, there was no significant change. CM had higher IP levels before and after infection as compared to CCR (Fig. 2). Cis-zeatin (cZ) decreased after infection in CM, while no significant variation was noted in the case of CCR. In contrast, trans-zeatin (tZ) levels highly

decreased in CCR as compared to CM in response to infection (Fig. 2). Overall, we noticed that CM had higher contents of auxins and cytokinins than CCR except for IBA and tZ.

P. brassicae infection was associated with a decreased in JA contents in *B. rapa* roots (Fig. 2). However, the levels of dihydro-Jasmonic acid (H2JA) and methyl Jasmonate (MEJA) increased in CM after *P. brassicae* infection. Levels of SA and 1-aminocyclopropanecarboxylic acid (ACC) were clearly different in both genotypes. We noticed a decrease of SA and ACC in CM after infection, while increased SA and ACC contents were observed in CCR (Fig. 2).

B. rapa root metabolome in response to *P. brassicae* infection

Using ESI-Q TRAP-MS/MS metabolite-profiling build upon the widely-targeted approach enabled the unambiguous structural characterization of 407 components belonging to 26 different classes according to the Metabolomics Standard Initiative (Fiehn et al., 2007). Compounds characterized by ESI-Q TRAP-MS/MS comprised a range of metabolites of which the most prevalent ones were phenolic acids, amino acids and derivatives, glucosinolates (GSLs), nucleotides, and derivatives, organic acids, fatty acids, and saccharides and alcohols. Chemical variation extended to additional classes of compounds, including flavonols, alkaloids, flavonoids, vitamins, lignans, plumerane, dihydroflavone, and dihydroflavonols. A total of 262 metabolites were differentially accumulated (DAM) between CM (infected samples) and CM-CK (control)

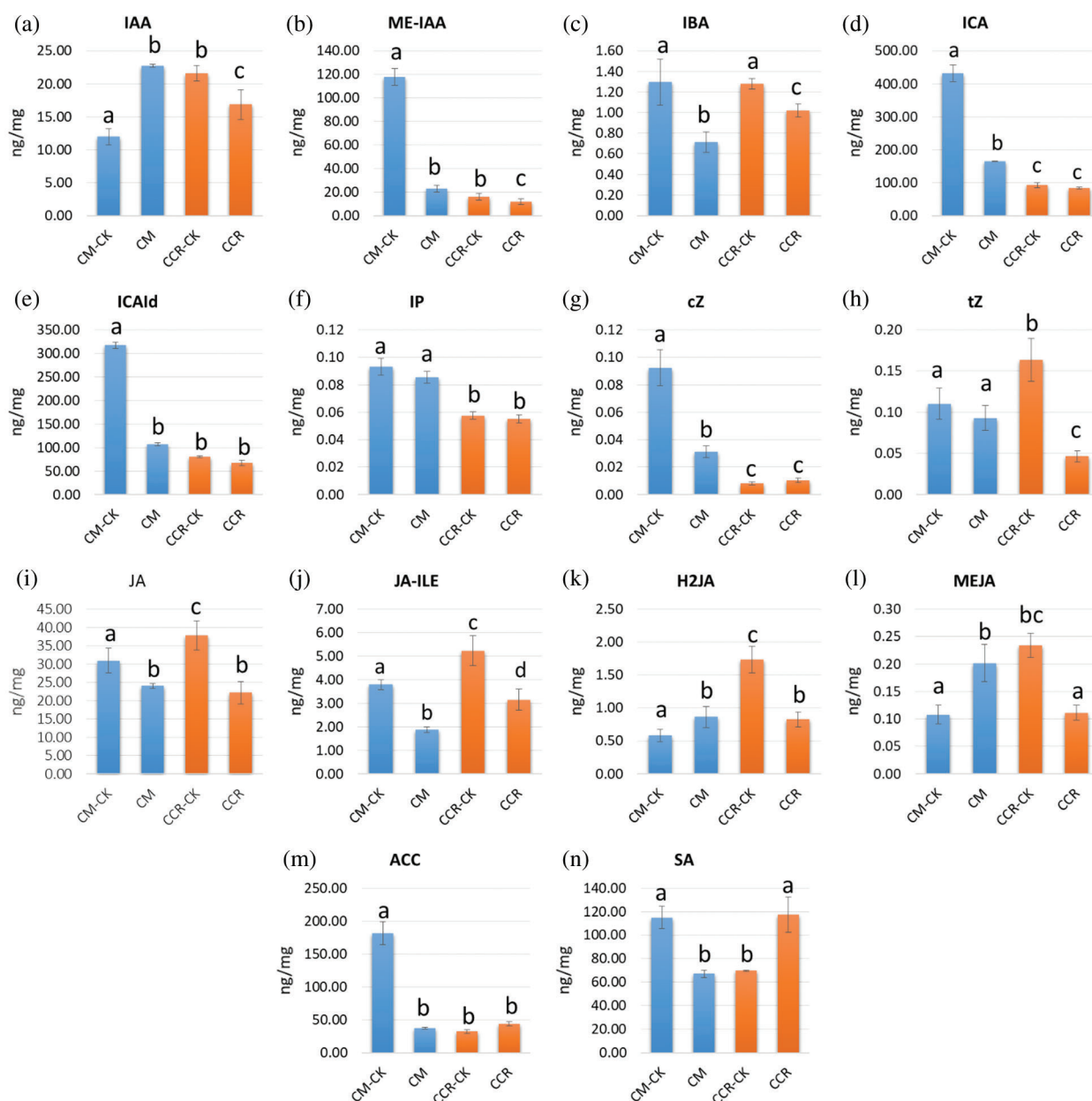


FIGURE 2. Phytohormone levels in susceptible (CM) and resistant (CCR) *B. rapa* genotypes before and at a late stage of infection (28 days) with *Plasmodiophora brassicae*.

IAA–Indole-3-acetic acid, ME-IAA–Methyl indole-3-acetate, IBA–3-Indolebutyric acid, ICAld–Indole-3-carboxaldehyde, ICA–Indole-3-carboxylic acid, IP–N-6-Isopentenyladenine, cZ–cis-zeatin, tZ–trans-zeatin, JA–Jasmonic acid, JA-ILE–Jasmonoyl-L-Isoleucine, H2JA–dihydrojasmonic acid, MEJA–methyl Jasmonate, ACC–1-Aminocyclopropanecarboxylic acid, SA–salicylic acid. Different letters (a, b) on the bars indicate significantly different values

(Additional Tab. 1), of which 128 were accumulated in higher quantities in CM. Thirteen metabolites were exclusively present in CM-CK, while 19 metabolites were exclusively accumulated in CM, suggesting that these metabolites play important role in responses to *P. brassicae* infection in the susceptible genotype (Fig. 3). A relatively lower number of metabolites (223) was differentially accumulated between CCR (infected samples) and CCR-CK (control), with 109 up-accumulated metabolites in CCR (Additional Tab. 2). We observed 14 and 9 metabolites that were exclusively accumulated in CCR-CK and CCR, respectively (Fig. 4).

Kyoto Encyclopedia of Genes and Genomes (KEGG) pathway enrichment analysis of the DAMs showed that

phenylpropanoid biosynthesis, ubiquinone, and other terpenoid-quinone biosynthesis, thiamine metabolism, vitamin B6 metabolism, and biotin metabolism were significantly enriched between CM-CK and CM (Fig. 5a). The metabolites in CCR-CK and CCR were significantly enriched in pathways related to arginine biosynthesis, biosynthesis of amino acids, lysine biosynthesis, fatty acid biosynthesis, and ABC transporters (Fig. 5b). Similarly, DAMs that were accumulated between both genotypes upon infection were enriched in glutathione metabolism, glucosinolate metabolism, fatty acid biosynthesis, and different amino acid biosynthetic pathways, i.e., arginine and proline metabolism and phenylalanine metabolism (Fig. 5c).

Compounds	CM-CK	CM	Log2FC
S-Allyl-L-cysteine	145500	9	-13.98
Leucylphenylalanine	9	63992.33	12.8
Glutathione reduced form	9	124713.33	13.76
Alanylleucine	9	385536.67	15.39
Delphinidin 3-O-glucoside (Mirtillin)	9	45756	12.31
Isobavachalcone D	954736.67	9	-16.69
Orychopramarin A[7,8-dihydroxy-3-(4-hydroxyphenyl)-isocoumarin]	838953.33	9	-16.51
Orychopramarin B[4,7-dihydroxy-3-(4-hydro_x005f_x005F_x0002_xyphenyl)-isocoumarin]	204360	9	-14.47
Pinocembrin(Dihydrochrysin)	1121600	9	-16.93
Saponarin 4'-O-glycoside	9	19106.33	11.05
Tricin 5-O-Glucoside	9	36570.33	11.99
Quercetin-3-O-(2"-galloyl)-β-D-glucoside	9	4016.9	8.8
3,7-Di-O-methylquercetin	9	13119.4	10.51
Isorhamnetin-hexose-malonate	9	68768.33	12.9
5(S),6(R)-Lipoxin A4	17052	9	-10.89
1,18-Octadecanediol	9	1907.23	7.73
5-Hexenyl Glucosinolate	40101.67	9	-12.12
1-Sulfo-indol-3-ylmethyl Glucosinolate (Glucobrassicin-1-sulfate)	9	8046.37	9.8
8-(Methylsulfonyl)octyl glucosinolate	9	27059	11.55
Glucosinalbin	9	37091.33	12.01
6-(3,4-Dihydroxyphenylacetic acid)-β-D-1-Glucosinolate of 4-(Methylsulfinyl)-3-butenyl	9	65139	12.82
1-Methylpropyl glucosinolate	9	474046.67	15.68
Isoquinoline	765633.33	9	-16.38
1-Methylxanthine	140103.33	9	-13.93
8-Hydroxy-2-deoxyguanosine	78979	9	-13.1
Phosphoenolpyruvic acid	9	44001.33	12.26
p-Hydroxyphenyl acetic acid	249883.33	9	-14.76
Bis(2-ethylhexyl)phthalate	176770	9	-14.26
4-Aminobenzoic acid	44695.33	9	-12.28
p-Coumaroylferuloyltartaric acid	9	52066	12.5
D-(+)-Melezitose	9	8564.03	9.89
Pyridoxal 5'-phosphate	9	123473.33	13.74

FIGURE 3. Differentially accumulated metabolites that were exclusively expressed in *P. brassicae* infected (CM) and control (CM-CK) samples.

We inputted “9” as the value for non-detected metabolites. The red and green bars show down- and up-accumulated metabolites in *P. brassicae* infected CM genotype, respectively.

Conserved and differential chemical signatures between susceptible and resistant genotypes

Comparison of the DAMs between the two genotypes showed that 132 metabolites were commonly regulated by *P. brassicae* in CCR_vs_CCR-CK and CM_vs_CM-CK, indicating that these metabolites represent the core-conserved metabolites altered in response to the pathogen, regardless of the genotype (Fig. 6; Additional Tab. 3). These metabolites belong to phenolic acids (26), amino acids and derivatives (18), glucosinolates (15), organic acids (11), flavonoids (12) nucleotides and derivatives (8), and fatty acids (8). Additional classes of metabolites included alkaloids (4), lignans and coumarins (5), vitamins (4), saccharides and alcohols (6), and phenolamines (4), and others. These are in accordance with earlier studies, which advocated the defensive role of the pathways related to these metabolites, i.e., amino acid biosynthesis, GSL biosynthesis, fatty acid biosynthesis, elongation, and degradation, GLT biosynthesis, and flavonoid biosynthesis (Frendo et al., 2013; Gullner et al., 2018; Ishida et al., 2014; Lim et al., 2017; Zeier, 2013;

Zhang et al., 2016; Zhu et al., 2013). Intriguingly, we observed that 72 out of these 132 core conserved metabolites were regulated in a contrasting pattern between CCR and CM, which may be a crucial resistance mechanism in CCR (See DAMs highlighted yellow in Additional Tab. 3). Furthermore, we observed 130 and 91 specific DAMs to CM and CCR, respectively, which may increase the susceptibility or resistance in the corresponding genotypes (Fig. 6; See highlighted yellow DAMs in Additional Tabs. 1 and 2, respectively). The unique DAMs in CM were classified as amino acids and derivatives (12 down- and 6 up-accumulated), anthocyanins (up-accumulated), chalcones (down-accumulated), coumarins (2 up- and 2 down-accumulated), dihydroflavones (down-accumulated), flavonoids (4 down- and 3 up-accumulated), free fatty acids (9 down- and 1 up-accumulated), glucosinolates (3 down- and 8 up-accumulated), lignans (1 down- and 2 up-accumulated), nucleotides and derivatives (12 down- and 4 up-accumulated), organic acids (2 down- and 4 up-accumulated), and phenolic acids (12 down- and 14

Compounds	CCR-CM	CCR	Log2FC
L-Tyramine	24854	9	-11.43
Crychophramarin A[7,8-dihydroxy-3-(4-hydroxyphenyl)-isocoumarin]	9	7606.7	9.72
Myricetin-3-O-rhamnoside (Myricitrin)	97916	9	-13.41
Quercetin-3-O-(2"-galloyl)-β-D-glucoside	13680.33	9	-10.57
5(S),6(R)-Lipoxin A4	9	5614.53	9.29
(Methylthio)hexyl glucosinolate	2673733.33	9	-18.18
4-Methylamyl Glucosinolate	1570700	9	-17.41
4-Methylpentyl Glucosinolate	1501400	9	-17.35
6-Heptenyl Glucosinolate	93393.33	9	-13.34
7-(Methylsulfinyl)Heptyl Glucosinolate	9	866250	16.55
Cytidine 5'-monophosphate(Cytidylic acid)	414423.33	9	-15.49
Citric acid	93379000	9	-23.31
2-Hydroxybutanoic acid	113934	9	-13.63
3-Hydroxy-3-methyl butyric acid	75313.67	9	-13.03
Methyl Anthranilate	9	13138.33	10.51
UROCANIC ACID(RG)	9	164543.33	14.16
N-hexosyl-p-coumaroyl putrescine	16031.67	9	-10.8
Tyrosol	18154	9	-10.98
2-O-Di-gallic acyl-β-D-Glucopyranoside-β-D-Glucopyranoside	15309.67	9	-10.73
4-Aminobenzoic acid	9	17927	10.96
3-Aminosalicylic acid	9	84924.33	13.2
Galloyl Methyl gallate	9	42320	12.2
4-Pyridoxic acid O-hexoside	9	5358.33	9.22

FIGURE 4. Differentially accumulated metabolites that were exclusively expressed in *P. brassicae* infected (CCR) and control (CCR-CK) samples. We inputted “9” as the value for non-detected metabolites. The red and green bars show down- and up-accumulated metabolites in *P. brassica* infected CCR genotype, respectively.

up-accumulated). Interestingly, the saccharides and alcohols were up-accumulated in response to infection. Though the DAMs specific to CM were higher than in CCR, we found that CCR had a higher ratio of up-accumulated DAMs after infection, belonging to classes such as amino acids and derivatives, free fatty acids, glucosinolates, and nucleotides and derivatives (see highlighted DAMs in [Additional Tab. 2](#)). These observations suggest that the susceptible genotype recruits more resources towards defense as compared to the resistant one, and the resistant genotype achieves resistance by inducing essential pathways enlisted above.

Differentially regulated pathways upon infection in CCR and CM

To further get insight into the difference in the metabolic changes after infection between both genotypes, we compared the metabolite ion intensity between CCR and CM at 28 DPI. In total, 240 DAMs were identified including, 138 and 102 down- and up-accumulated metabolites in CCR ([Additional Tab. 4](#)). The most significantly enriched pathways were fatty acid biosynthesis followed by galactose metabolism, 2-oxocarboxylic acid metabolism, pantothenate and CoA biosynthesis, amino acid pathways (phenylalanine metabolism and arginine and proline metabolism), glycolysis/gluconeogenesis, and glucosinolate biosynthesis. An important part of 2-oxocarboxylic acid metabolism is glucosinolate biosynthesis, which is discussed in the glucosinolate metabolism subsection. Among other pathways, the galactose metabolism pathway showed a significant accumulation of D-glucose in CCR as compared to CM. This was possibly due to the increased synthesis of melibiose; melibiose conversion to D-glucose is catalyzed by alpha-galactosidase (EC 3.2.1.22). The same enzyme is implicated in the production of D-myoinositol in this pathway ([Additional Fig. 1](#)). D-glucose

accumulation was also shown in glycolysis/gluconeogenesis, starch, and sucrose metabolism as well as in the pentose phosphate pathway. The myoinositol is then converted into L-ascorbate in ascorbate and alderate metabolism, which further influences xylitol and D-arabitol. These metabolites then take part in riboflavin metabolism and ultimately produce flavin adenine dinucleotide (FAD) ([Additional Figs. 1–4](#)). The metabolic changes in other significantly enriched pathways are given below.

Fatty acid biosynthesis

Metabolites related to fatty acid biosynthesis, elongation, degradation, metabolism, and biosynthesis of unsaturated fatty acid were differentially accumulated between both genotypes. Hexadecanoic acid, which is involved in fatty acid elongation and fatty acid metabolism, was accumulated in higher quantity in CCR as compared to CM (log2 fold change = 1.44). Similarly, palmitic acid, which is also involved in fatty acid metabolism, was significantly up-accumulated in CCR as compared to CM (log2 fold change = 2.44). While lauric acid, which is involved in fatty acid degradation, was down-accumulated in CCR as compared to CM (log2 fold change = -1.31). These observations suggest that the resistant genotype increases the biosynthesis and elongation of fatty acids as a resistance mechanism. A similar observation has been made in *Arabidopsis*, where several fatty acid syntheses and elongation related genes were upregulated in plants infected with *P. brassicae* pathotype P3 ([Irani et al., 2018](#)). The authors suggested that this could be linked to the accumulation of lipid droplets in plasmodia in infected root cells ([Additional Tab. 4; Fig. 7](#)).

Amino acid biosynthesis

Regulation of amino acid metabolism, in response to clubroot infection and disease progression, has been previously

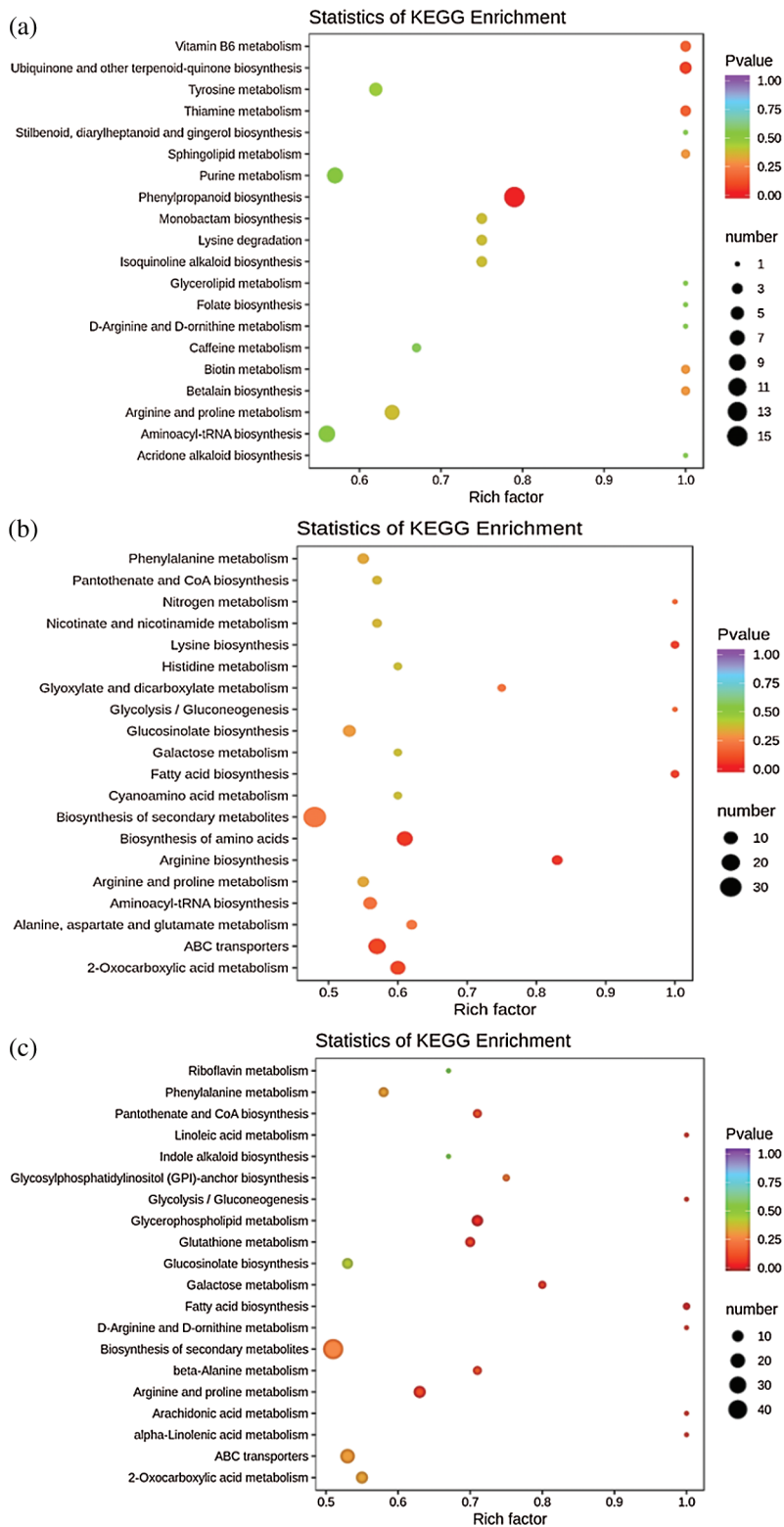


FIGURE 5. KEGG pathway enrichment analyses between (a) CM-CK and CM, and (b) CCR-CK and CCR.

CM-susceptible genotype (infected), and (c) infected CM and infected CCR. CCR-resistant genotype (infected), and CK-control

reported (Chiang and Nip, 1971; Wagner et al., 2012). L-histidine and L-arginine biosynthesis was significantly increased in CCR as compared to CM (\log_2 fold change = 3.04 and 3.82, respectively). Similarly, we noticed the increased biosynthesis of L-proline, L-citrulline, and L-aspartic acid in CCR (\log_2 fold change = 2.55, 2.43, and 2.31, respectively). Among other amino acid biosynthesis-related metabolites, anthranilic acid was accumulated in CCR (\log_2 fold change = 1.67). It is a phenolic acid and is

an important metabolite for tryptophan production. Tryptophan did not differentially accumulate between both genotypes upon infection. However, 5-hydroxytryptophol, which is produced from tryptophan, was highly accumulated in CCR than CM. *Arabidopsis* infected with clubroot disease also showed the upregulation of transcripts related to tryptophan (Irani et al., 2018). O-acetylserine was less accumulated in the resistant genotype than the susceptible one (\log_2 fold change = -1.13).

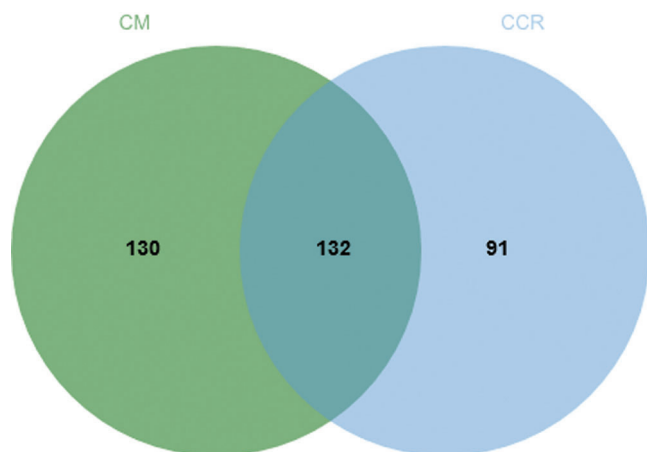


FIGURE 6. Venn diagram representing the number of differentially accumulated metabolites (DAM) in CCR_vs_CCR-CK and CM_vs_CM-CK.

The overlapping area in the diagram represents the number of DAMs that were common in both genotypes

2,6-Diaminoimelic acid, which is involved in the formation of lysine, was highly accumulated in CCR (log₂ fold change = 1.84). Interestingly, citric acid was strongly down-accumulated in CCR (log₂ fold change = -23.30). This suggests that citric acid repression plays an important role in resistance against *P. brassicae* infection. Another metabolite, i.e., 3-methyl-2-oxobutanoic acid was less accumulated in CCR as compared to CM (log₂ fold change = -1.46) (Additional Tabs. 1, 2, and 4; Fig. 8).

Glutathione metabolism

Glutathione (GLT) transferase is important in response to disease infection, which can catalyze the combination of GLT and other electrophilic compounds to protect plants against pathogens (Fei *et al.*, 2016; Frendo *et al.*, 2013). In the earlier report on the proteome of the clubroot infected *B. rapa* roots, it was observed that GLT reductase production was stimulated at 28 and 35 DPI (Lan *et al.*, 2019). Similarly, we noticed that the KEGG pathways analysis showed metabolites enriched in GLT metabolism. Glutathione (reduced form, i.e., thiol-reduced) was accumulated in higher quantity in CCR as compared to CM

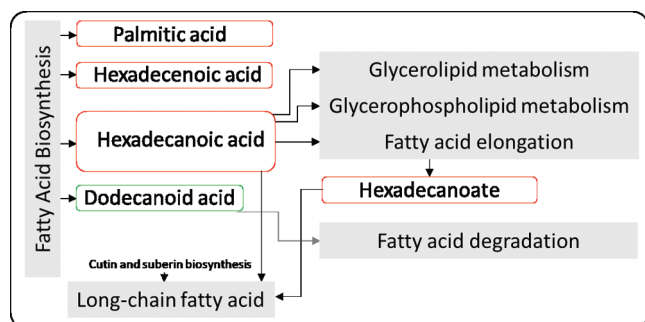


FIGURE 7. Regulation of metabolites related to fatty acid-related pathways.

Red boxes show the metabolites that are up-accumulated in resistant genotype-CCR, while the green box shows the metabolites that are up-accumulated in susceptible genotype-CM

(log₂ fold change = 1.41). The other form, i.e., oxidized GLT (disulfide-oxidized (GSSG)) was also highly accumulated in CCR (log₂ fold change = 1.96). Additionally, we noticed the increased accumulation of spermidine and ascorbate in CCR as compared to CM during *P. brassicae* infection (Fig. 9; Additional Tabs. 1, 3, and 4).

Glucosinolate metabolism

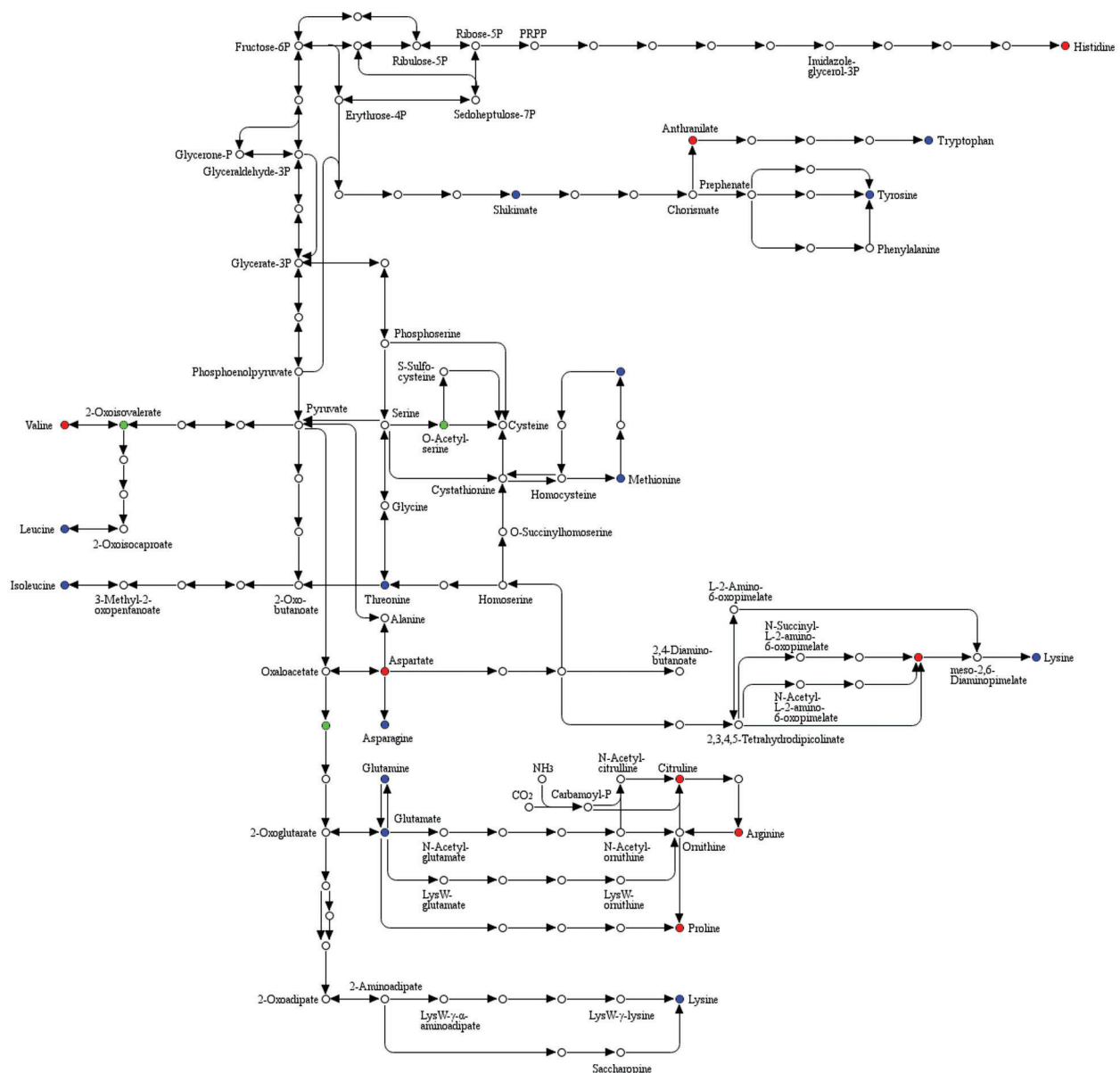
Glucosinolates (GSLs) are secondary metabolism products in Brassicaceae and have been regarded as defense compounds against clubroot as well as general pathogens and insects (Ludwig-Müller *et al.*, 2009). A comparison between both infected genotypes showed that 33 metabolites, classified as GSLs, were differentially accumulated (Additional Tab. 4). Nine of these metabolites were accumulated in CM in higher quantities while 24 were higher accumulated in CCR. These observations suggest that the resistant genotype, i.e., CCR, had increased production of GSLs in response to infection at the studied time point. According to Halkier and Gershenzon (2006), GSLs are of three types, i.e., aliphatic (derived from methionine), aromatic (derived from tyrosine and phenylalanine, and indolic forms (derived from tryptophan). The GSL DAMs accumulated between the infected CCR and CM belonged to all three classes, suggesting that this pathway has an important role in the resistance mechanism in CCR (Fig. 10).

Discussion

Divergent responses of auxins and cytokinins in P. brassicae infected B. rapa

For many years, the interest has been paid to the role of auxins in hypertrophied root formation after the infection with *P. brassicae*. Auxin levels (particularly IAA) have been studied in infected roots on different DPI by different researchers (Devos *et al.*, 2005), which revealed that the level of auxins is non-synchronized. Particularly on 28 DPI, lower levels of IAA have been detected in infected roots than control (Kavanagh and Williams, 1981). We observed this in the case of the resistant genotype; however, the susceptible genotype showed almost double the IAA levels after infection. This is consistent with the phenotypic changes in the roots as we did not notice any gall formation in the resistant genotype after the infection (Fig. 1), hence the gall formation in the susceptible genotype is possibly associated with the increased IAA levels after infection (Raa, 1971). Devos and Prinsen (2005) reported that a *de novo* meristematic area (gall) is established in the infected roots (in susceptible genotypes) that acts as a sink for host-derived IAA, carbohydrates, nitrogen, and energy to maintain the pathogen and to trigger gall development. Furthermore, it was previously reported that gall formation requires cell division and cell elongation, for which IAA plays an important role (Devos *et al.*, 2005). Additionally, the work on *Arabidopsis* has provided evidence for the involvement of auxin-signaling pathways for the establishment of the root galls by *P. brassicae* (Jahn *et al.*, 2013). Gall formation in many plant-microbe interactions can be triggered by alterations in either auxin and/or cytokinin metabolism (Robin *et al.*, 2019). Data on

BIOSYNTHESIS OF AMINO ACIDS



01230 2/1/19
© Kanehisa Laboratories

FIGURE 8. Biosynthesis of amino acids pathway showing differentially accumulated metabolites between *P. brassicae* infected susceptible (CM) and resistant (CCR) *B. rapa* genotypes. Red—significantly up-accumulated, green—significantly down-accumulated, and blue—detected but not significantly accumulated

cytokinin levels in the clubroot infected plants is relatively consistent than auxins. Previously, it was shown that enhanced degradation of cytokinins in plants causes resistance to pathogens (Armstrong, 1994; Kakimoto, 2001). This was visible in both genotypes, where the disease infection resulted in a reduction in the cytokinin levels. The resistant genotype—CCR showed relatively lower levels of IP and cZ as compared to CM, which is possibly due to the fact that the resistant genotype had higher cytokinins degradation (Fig. 2). Studies on *Arabidopsis* have reported that this degradation could be associated with the expression of genes encoding cytokinin oxidase/dehydrogenases, which are responsible for cytokinin degradation (Siemens et al., 2006).

Role of defense responsive phytohormones—Jasmonic acid, salicylic acid, and ethylene

Earlier studies led the general conceptual model where combined action of hormonal pathways has been implicated in response to pathogens. Particularly it was noted that SA-mediated defenses and JA/ethylene-dependent defenses inhibit different pathogens in plants (Glazebrook, 2005; Thomma et al., 1998). In this regard, some recent studies assessed the contribution of both SA and JA to basal and partial resistance in *Arabidopsis* and *Brassica napus* by studying the phytohormone levels and the expression of related genes in clubroot resistant and resistant genotypes at different DPI (Lemarié et al., 2015; Prerostova et al., 2018). The jasmonic acid content in partially resistant and

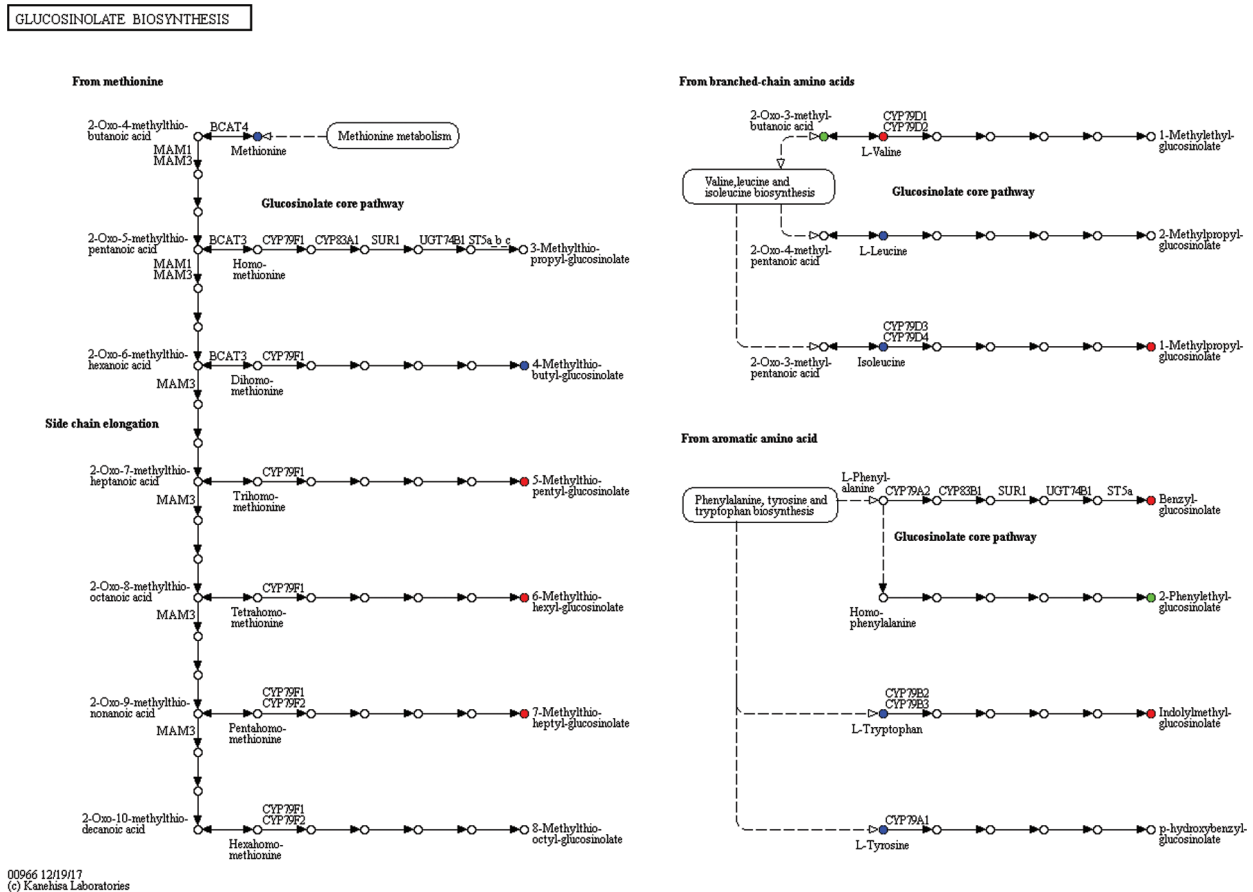


FIGURE 10. Glucosinolate metabolism pathway showing differentially accumulated metabolites between *P. brassicae* infected susceptible (CM) and resistant (CCR) *B. rapa* genotypes. Red—significantly up-accumulated, green—significantly down-accumulated, and blue—detected but not significantly accumulated

The role of ethylene in resistance to clubroot has been shown in plants (Knaust and Ludwig-Müller, 2013; Lahlali et al., 2014). *Arabidopsis* mutants for ethylene were tested against susceptibility to clubroot, which showed an altered degree of susceptibility (Knaust and Ludwig-Müller, 2013). Our results that the levels of ACC did not change in the resistant genotype could be due to the genetic background of the genotype. For example, ethylene receptor mutant (*etr1-3*) was more susceptible than wild type *Arabidopsis*, while ethylene insensitive mutant (*ein5-1*) showed a tolerant phenotype (Devos and Prinsen, 2005).

Increased glucose accumulation in resistant B. rapa genotype—does it have a role in resistance?

Endogenous changes in glucose levels have long been associated with the enhancement of resistance to fungal pathogens in plants (Morkunas and Ratajczak, 2014). The increased biosynthesis of sucrose in the resistant genotype (CCR) could suggest that sugar signals in CCR probably function as priming molecules leading to pathogen-associated molecular patterns-triggered immunity or so-called sweet priming as reported earlier (Bolouri Moghaddam and Van den Eden 2012). It has been suggested that an enhanced supply of sugars may cause an increase in respiration and reactive oxygen species production, and thus increasing resistance (Morkunas and

Bednarski, 2008). We also noticed that as a part of galactose metabolism (and inositol phosphate metabolism), myoinositol was also up-accumulated in CCR. This directly affects the higher production of L-gulonono-1,4-lactone, which is then converted into L-ascorbate. The increased accumulation of L-ascorbate possibly influenced xylitol and D-arabitol accumulation in CCR (Additional Figs. 2 and 3). There is a possibility that these metabolites can take part in riboflavin metabolism since this pathway is present downstream of the xylitol and D-arabitol (Additional Fig. 4). We found that FAD was up-accumulated in CCR in this pathway, which is a very strong oxidizing agent (FAD^+) as well as an important prosthetic group for several enzymes participating in redox reactions (Asai et al., 2010). Based on these metabolome changes, it is proposed that glucose accumulation in CCR could be one strategy for resistance against *B. brassicae* infection.

Fatty acid biosynthesis and elongation—role in defense against P. brassicae

Being the essential constituents of plant cells, fatty acids, and lipids are involved in structural integrity as well as sources of energy for various metabolic processes. However, their role as signal transduction mediators as intra- and extracellular signals is well established when plants are infected by pathogens (Kachroo and Kachroo, 2009; Lim et al., 2017).

Recent findings also indicated the essential role of very-long-chain fatty acids with plant defense through different aspects (Raffaele *et al.*, 2009). The higher accumulation of metabolites involved in cutin, suberin, and wax biosynthesis is consistent with the previous report in *Arabidopsis* roots, where the up-regulation of many genes related to lipid biosynthesis and elongation was reported (Irani *et al.*, 2018; Raffaele *et al.*, 2009). Some researchers have associated this increased lipid reserves in the infected roots to satisfy pathogen lipid demand (Irani *et al.*, 2018). However, this could be true in the case of the susceptible genotypes which have the galls and resting spores (Siemens *et al.*, 2006). Nevertheless, the accumulation of metabolites that are involved in lipid biosynthesis and fatty acid elongation is possibly the defense response in the resistant genotype. This increased accumulation could be either due to the up-regulation of genes belonging to elongase complexes or increased lipid transport in the sites of infection (Raffaele *et al.*, 2009; Zhu *et al.*, 2013). On the contrary, to increased accumulation of these metabolites, the decreased accumulation (down-regulation) of metabolites associated with fatty acid degradation in CCR and the opposite in CM suggests that the resistant genotype keeps their pools of fatty acids by increased biosynthesis as well synthesizing long-chain fatty acids and reducing their degradation (Kachroo and Kachroo, 2009). However, it is not always true because breakdown products of fatty acids result in the production of cyclic or acyclic oxidation products, i.e., oxylipins, which participate in plant defense by performing signaling functions (Blée, 2002).

Amino acids and glucosinolates play role in defense against P. brassicae

Glucosinolates are the secondary metabolites that are commonly present in members of the order Brassicales. It is well established that GSLs and their degradation products play important roles in plants against fungal and bacterial pathogens (Barth and Jander, 2006; Bednarek *et al.*, 2009; Fan *et al.*, 2011). Since GSLs are classified into three categories based on their precursor amino acids, signifying that amino acids have a pivotal role in the biosynthesis of plant products, which consequently affect the plant immune system (Halkier and Gershenzon, 2006). Apart from the diverse constitutive and inducible defense pathways regulated by classical phytohormones and defense-related proteins, distinct amino acid metabolic pathways are integral parts of the plant's strategy to combat pathogens (Zeier, 2013). Different studies on clubroot proteome and transcriptome have reported the involvement of different amino acid pathways in *Arabidopsis* and brassicas (Fu *et al.*, 2019; Irani *et al.*, 2018; Lan *et al.*, 2019). The higher aliphatic GSLs, i.e., 5-methylthio-pentyl-GSL, 6-methylthio-pentyl-GSL, and 7-methylthio-pentyl-GSL, accumulation in CCR indicated that side-chain elongation is active which is under the control of cytochromes P450 (CYP79F1/F2) and MAMs (methylthioalkylmalate synthases) (Bednarek *et al.*, 2009; Ishida *et al.*, 2014). It is important to mention here that the higher accumulation of 5-hydroxytryptophol, which is produced from tryptophan, in CCR could indicate that tryptophan is converted by the action of indole GSL genes

(Hull *et al.*, 2000). A similar report was found in *Arabidopsis* where the infected roots also showed the upregulation of transcripts related to tryptophan. Furthermore, the same result was observed in a previous report in *B. rapa* by using the proteome analysis approach (Lan *et al.*, 2019). The up-regulation of gluco-brassicin (a common indole GSL) in CCR indicates its important role in defense against *P. brassicae*. Previously, increased accumulation of novel GSLs has been associated with the modulation of disease resistance in plants (Brader *et al.*, 2006). The GSL derived from branched-chain amino acids, i.e., 1-methylpropyl-GSL accumulated in CCR in higher quantity as compared to CM. This is consistent with the increased accumulation of L-valine in CCR (Additional Tab. 4). L-valine is an important metabolite in this pathway as it takes part in the production of GSLs (Fig. 9). Finally, the higher accumulation of benzyl-GSL (CRR and CM), indolylmethyl-GSL (CCR), cyclobrassicin (CCR), glucobrassicin-1-sulfate (CCR and CM), 4-hydroxyglucobrassicin (CRR) clearly indicates that CCR alters its GSL profiles to modulate clubroot resistance at the studied time period to a better extent as compared to CM (Additional Tabs. 1–4). This increased accumulation of GSL can be either due to the increased accumulation of respective amino acid residues or up-regulation of genes involved in GSL biosynthesis pathways (Ludwig-Müller, 2009). As we analyzed the metabolites, it could be therefore stated that amino acid biosynthesis leads the increased GSL accumulation in CCR, leading to resistance against clubroot (Yan and Chen, 2007).

Role of glutathione in B. rapa resistance against P. brassicae

Glutathione plays a crucial role in plant antioxidative defense by limiting the excessive spread of hypersensitive response-associated cell death (Franco and Cidlowski, 2012; Levine *et al.*, 1994). Glutathione has long been associated with the plants' ability to defend against different types of pathogens in different crops ranging from biotrophic, hemibiotrophic, and necrotrophic fungi to bacterial and viral pathogens. Furthermore, its role in basal resistance and R-gene mediated resistance is well established. Elevated GLT levels, as well as marked accumulation of GLT proteins and transcripts, have been reported in different plant-pathogen interactions (Gullner *et al.*, 2018). The proteome analysis of CM and CCR had previously shown the accumulation of GLT protection against *P. brassicae* (Lan *et al.*, 2019). Since, in this study, we found GST (both oxidized and reduced forms) accumulated in response to infection in both the susceptible and resistant genotypes at 28 DPI, it could be therefore stated that GLT plays important defense responsive functions against *P. brassicae* regardless of the genetic background of the genotype. This increase in GLT production is typical in many defense responses e.g., hypersensitive response in tobacco mosaic virus-infected plants, *Pseudomonas syringae* pv. *Glycinea* infected plants, and powdery mildew infection in plants (Mauch and Dudler, 1993; Tenhaken *et al.*, 1995; Juhasz and Gullner, 2014). These studies suggested that GLT plays a role as an antioxidant as well as a signaling agent contribution to plant disease resistance (Gullner *et al.*, 2017). It is important to

note that since we detected higher GLT levels in CCR, it could be therefore stated that the resistant genotype employs this pathway by increased GLT production. Future studies on the major signals that play a role in the elevation of GLT by triggering the expression of GLT synthesis-related enzymes will shed light on specific steps involved in resistance development.

Supplementary Material: Supplementary materials are available online at DOI: 10.32604/biocell.2020.012954.

Author Contribution: ML and JH conceived the study and designed the experiments. ML, JH, HY, LZ, and XX performed the experiments. JH provided funding and supervised the study. ML, JH, and HY analyzed the data. XX and JH were involved in obtaining the materials. ML wrote the manuscript with contributions from the other authors. All authors have read and approved the final version of the manuscript.

Availability of Data and Materials: All the data is provided in the manuscript and or supplementary material. For plant material no voucher has been deposited in a genebank.

Funding Statement: This research was supported by the National Bulk Vegetable Industry Technology System of China (CARS-23-G37), Research and integrated demonstration of green key technologies of main export vegetables in Yunnan Province (2019ZG001), Yunnan Province “ten thousand talents plan” Yunling industrial technology leading talents, Special support of Modern Agricultural Technology Department of vegetables in Yunnan Province. The funder has no role in study design, data collection and analysis, decision to publish, or preparation of the manuscript.

Conflict of Interest: The authors declare that they have no conflicts of interest to report regarding the present study.

References

- Armstrong DJ (1994). *Cytokinin Oxidase and the Regulation of Cytokinin Degradation. Cytokinins: Chemistry, Activity, and Function*. Boca Raton, FL: CRC Press, 139-154.
- Asai S, Mase K, Yoshioka H (2010). A key enzyme for flavin synthesis is required for nitric oxide and reactive oxygen species production in disease resistance. *Plant Journal* **62**: 911-924.
- Barth C, Jander G (2006). *Arabidopsis* myrosinases TGG1 and TGG2 have redundant function in glucosinolate breakdown and insect defense. *Plant Journal* **46**: 549-562. DOI 10.1111/j.1365-313X.2006.02716.x.
- Bednarek P, Piślewska-Bednarek M, Svatoš A, Schneider B, Doubský J, Mansurova M, Humphry M, Consonni C, Panstruga R, Sanchez-Vallet A, Molina A, Schulze-Lefert P (2009). A glucosinolate metabolism pathway in living plant cells mediates broad-spectrum antifungal defense. *Science* **323**: 101-106. DOI 10.1126/science.1163732.
- Blée E (2002). Impact of phyto-oxylipins in plant defense. *Trends in Plant Science* **7**: 315-322. DOI 10.1016/S1360-1385(02)02290-2.
- Brader G, Mikkelsen MD, Halkier BA, Tapio Palva E (2006). Altering glucosinolate profiles modulates disease resistance in plants. *Plant Journal* **46**: 758-767. DOI 10.1111/j.1365-313X.2006.02743.x.
- Chai A, Xie X, Shi Y, Li B (2014). Research status of clubroot (*Plasmodiophora brassicae*) on cruciferous crops in China. *Canadian Journal of Plant Pathology* **36**: 142-153. DOI 10.1080/07060661.2013.868829.
- Chiang M, Nip W (1971). Free amino acids content in root tissue of clubroot resistant and susceptible cabbages. *Canadian Journal of Plant Science* **51**: 66-67. DOI 10.4141/cjps71-013.
- Chong J, Xia J (2018). MetaboAnalystR: An R package for flexible and reproducible analysis of metabolomics data. *Bioinformatics* **34**: 4313-4314. DOI 10.1093/bioinformatics/bty528.
- Cui K, Lin Y, Zhou X, Li S, Liu H, Zeng F, Zhu F, Ouyang G, Zeng Z (2015). Comparison of sample pretreatment methods for the determination of multiple phytohormones in plant samples by liquid chromatography-electrospray ionization-tandem mass spectrometry. *Microchemical Journal* **121**: 25-31. DOI 10.1016/j.microc.2015.02.004.
- Devos S, Prinsen E (2005). *Plant hormones: A key in clubroot development*: Universiteit Antwerpen, Faculteit Wetenschappen, Departement Biologie.
- Devos S, Vissenberg K, Verbelen JP, Prinsen E (2005). Infection of Chinese cabbage by *Plasmodiophora brassicae* leads to a stimulation of plant growth: Impacts on cell wall metabolism and hormone balance. *New Phytologist* **166**: 241-250. DOI 10.1111/j.1469-8137.2004.01304.x.
- Dixon GR (2009). The occurrence and economic impact of *Plasmodiophora brassicae* and clubroot disease. *Journal of Plant Growth Regulation* **28**: 194-202. DOI 10.1007/s00344-009-9090-y.
- Fan J, Crooks C, Creissen G, Hill L, Fairhurst S, Doerner P, Lamb C (2011). *Pseudomonas* sax genes overcome aliphatic isothiocyanate-mediated non-host resistance in *Arabidopsis*. *Science* **331**: 1185-1188. DOI 10.1126/science.1199707.
- Fei W, Feng J, Rong S, Strelkov SE, Gao Z, Hwang SF (2016). Infection and gene expression of the clubroot pathogen *Plasmodiophora brassicae* in resistant and susceptible canola cultivars. *Plant Disease* **100**: 824-828. DOI 10.1094/PDIS-11-15-1255-RE.
- Fiehn O, Robertson D, Griffin J, van der Werf M, Nikolau B, Morrison N, Sumner LW, Goodacre R, Hardy NW, Taylor C, Foster J, Kristal B, Kaddurah-Daouk R, Mendes P, van Ommen B, Lindon JC, Sansone SA (2007). The metabolomics standards initiative (MSI). *Metabolomics* **3**: 175-178. DOI 10.1007/s11306-007-0070-6.
- Franco R, Cidlowski JA (2012). Glutathione efflux and cell death. *Antioxidants & Redox Signaling* **17**: 1694-1713. DOI 10.1089/ars.2012.4553.
- Frendo P, Baldacci-Cresp F, Benyamina SM, Puppo A (2013). Glutathione and plant response to the biotic environment. *Free Radical Biology and Medicine* **65**: 724-730. DOI 10.1016/j.freeradbiomed.2013.07.035.
- Fu P, Piao Y, Zhan Z, Zhao Y, Pang W, Li X, Piao Z (2019). Transcriptome profile of *Brassica rapa* L. reveals the involvement of jasmonic acid, ethylene, and brassinosteroid signaling pathways in clubroot resistance. *Agronomy* **9**: 589. DOI 10.3390/agronomy9100589.
- Glazebrook J (2005). Contrasting mechanisms of defense against biotrophic and necrotrophic pathogens. *Annual Review of Phytopathology* **43**: 205-227. DOI 10.1146/annurev.phyto.43.040204.135923.
- Gullner G, Komives T, Király L, Schröder P (2018). Glutathione S-transferase enzymes in plant-pathogen interactions. *Frontiers in Plant Science* **9**: 1836. DOI 10.3389/fpls.2018.01836.

- Gullner G, Zechmann B, Kunstler A, Kiraly L (2017). The signaling role roles of glutathione in plant disease resistance. In: Hossain M, Mostofa M, Diaz-Vivancos P, Burritt D, Fujitt D, Fujita M, Tran LS, eds., *Glutathion in Plant Growth, Development, and Stress Tolerance*. Cham: Springer, 331–357.
- Halkier BA, Gershenzon J (2006). Biology and biochemistry of glucosinolates. *Annual Review of Plant Biology* **57**: 303–333. DOI 10.1146/annurev.arplant.57.032905.105228.
- Huang L, Yang Y, Zhang F, Cao J (2017). A genome-wide SNP-based genetic map and QTL mapping for agronomic traits in Chinese cabbage. *Scientific Reports* **7**: 46305. DOI 10.1038/srep46305.
- Hull AK, Vij R, Celenza JL (2000). *Arabidopsis* cytochrome P450s that catalyze the first step of tryptophan-dependent indole-3-acetic acid biosynthesis. *Proceedings of the National Academy of Sciences of the United States of America* **97**: 2379–2384. DOI 10.1073/pnas.040569997.
- Irani S, Trost B, Waldner M, Nayidu N, Tu J, Kusalik AJ, Todd CD, Wei Y, Bonham-Smith PC (2018). Transcriptome analysis of response to *Plasmodiophora brassicae* infection in the *Arabidopsis* shoot and root. *BMC Genomics* **19**: 23. DOI 10.1186/s12864-017-4426-7.
- Ishida M, Hara M, Fukino N, Kakizaki T, Morimitsu Y (2014). Glucosinolate metabolism, functionality and breeding for the improvement of Brassicaceae vegetables. *Breeding Science* **64**: 48–59. DOI 10.1270/jsbbs.64.48.
- Jahn L, Mucha S, Bergmann S, Horn C, Staswick P, Steffens B, Siemens J, Ludwig-Müller J (2013). The clubroot pathogen (*Plasmodiophora brassicae*) influences auxin signaling to regulate auxin homeostasis in *Arabidopsis*. *Plants* **2**: 726–749. DOI 10.3390/plants2040726.
- Juhász C, Gullner G (2014). The monoterpene (S)-carvone massively up-regulates several classes of glutathione S-transferase genes in tobacco leaf discs. *Acta Phytopathologica et Entomologica Hungarica* **49**: 163–176. DOI 10.1556/APhyt.49.2014.2.3.
- Kachroo A, Kachroo P (2009). Fatty acid-derived signals in plant defense. *Annual Review of Phytopathology* **47**: 153–176. DOI 10.1146/annurev-phyto-080508-081820.
- Kakimoto T (2001). Identification of plant cytokinin biosynthetic enzymes as dimethylallyl diphosphate: ATP/ADP isopentenyltransferases. *Plant and Cell Physiology* **42**: 677–685. DOI 10.1093/pcp/pce112.
- Kavanagh J, Williams P (1981). Indole auxins in *Plasmodiophora* infected cabbage roots and hypocotyls. *Transactions of the British Mycological Society* **77**: 125–129. DOI 10.1016/S0007-1536(81)80186-6.
- Kayum MA, Park J-I, Nath UK, Saha G, Biswas MK, Kim H-T, Nou I-S (2017). Genome-wide characterization and expression profiling of PDI family gene reveals function as abiotic and biotic stress tolerance in Chinese cabbage (*Brassica rapa* ssp. *pekinensis*). *BMC Genomics* **18**: 885. DOI 10.1186/s12864-017-4277-2.
- Knaust A, Ludwig-Müller J (2013). The ethylene signaling pathway is needed to restrict root gall growth in *Arabidopsis* after infection with the obligate biotrophic protist *Plasmodiophora brassicae*. *Journal of Plant Growth Regulation* **32**: 9–21. DOI 10.1007/s00344-012-9271-y.
- Kobelt P, Siemens J, Sacristán MD (2000). Histological characterisation of the incompatible interaction between *Arabidopsis thaliana* and the obligate biotrophic pathogen *Plasmodiophora brassicae*. *Mycological Research* **104**: 220–225. DOI 10.1017/S0953756299001781.
- Lahlali R, McGregor L, Song T, Gossen BD, Narisawa K, Peng G (2014). Heteroconium chaetospora induces resistance to clubroot via upregulation of host genes involved in jasmonic acid, ethylene, and auxin biosynthesis. *PLoS One* **9**: e94144. DOI 10.1371/journal.pone.0094144.
- Lan M, Li G, Hu J, Yang H, Zhang L, Xu X, Liu J, He J, Sun R (2019). iTRAQ-based quantitative analysis reveals proteomic changes in Chinese cabbage (*Brassica rapa* L.) in response to *Plasmodiophora brassicae* infection. *Scientific Reports* **9**: 12058. DOI 10.1038/s41598-019-48608-0.
- Lemarié S, Robert-Seilaniantz A, Lariagon C, Lemoine J, Marnet N, Jubault M, Manzaneres-Dauleux MJ, Gravot A (2015). Both the jasmonic acid and the salicylic acid pathways contribute to resistance to the biotrophic clubroot agent *Plasmodiophora brassicae* in *Arabidopsis*. *Plant and Cell Physiology* **56**: 2158–2168.
- Levine A, Tenhaken R, Dixon R, Lamb C (1994). H₂O₂ from the oxidative burst orchestrates the plant hypersensitive disease resistance response. *Cell* **79**: 583–593. DOI 10.1016/0092-8674(94)90544-4.
- Li L, Long Y, Li H, Wu X (2020). Comparative transcriptome analysis reveals key pathways and hub genes in rapeseed during the early stage of *Plasmodiophora brassicae* infection. *Frontiers in Genetics* **10**: 1275. DOI 10.3389/fgene.2019.01275.
- Lim GH, Singhal R, Kachroo A, Kachroo P (2017). Fatty acid- and lipid-mediated signaling in plant defense. *Annual Review of Phytopathology* **55**: 505–536. DOI 10.1146/annurev-phyto-080516-035406.
- Lovelock DA, Šola I, Marschollek S, Donald CE, Rusak G, van Pée KH, Ludwig-Müller J, Cahill DM (2016). Analysis of salicylic acid-dependent pathways in *Arabidopsis thaliana* following infection with *Plasmodiophora brassicae* and the influence of salicylic acid on disease. *Molecular Plant Pathology* **17**: 1237–1251. DOI 10.1111/mp.12361.
- Ludwig-Müller J (2009). Glucosinolates and the clubroot disease: Defense compounds or auxin precursors? *Phytochemistry Reviews* **8**: 135–148. DOI 10.1007/s11101-008-9096-2.
- Ludwig-Müller J, Prinsen E, Rolfe SA, Scholes JD (2009). Metabolism and plant hormone action during clubroot disease. *Journal of Plant Growth Regulation* **28**: 229–244. DOI 10.1007/s00344-009-9089-4.
- Ludwig-Müller J, Schuller A (2007). *What Can We Learn from Clubroots: Alterations in Host Roots and Hormone Homeostasis Caused by Plasmodiophora Brassicae Sustainable Disease Management in a European Context*. Dordrecht: Springer, 291–302.
- Ludwig-Müller J, Jülke S, Geiß K, Richter F, Mithöfer A, Šola I, Rusak G, Keenan S, Bulman S (2015). A novel methyltransferase from the intracellular pathogen *Plasmodiophora brassicae* methylates salicylic acid. *Molecular Plant Pathology* **16**: 349–364. DOI 10.1111/mpp.12185.
- Malinowski R, Novák O, Borhan MH, Spíchal L, Strnad M, Rolfe SA (2016). The role of cytokinins in clubroot disease. *European Journal of Plant Pathology* **145**: 543–557. DOI 10.1007/s10658-015-0845-y.
- Mauch F, Dudler R (1993). Differential induction of distinct glutathione-S-transferases of wheat by xenobiotics and by pathogen attack. *Plant Physiology* **102**: 1193–1201. DOI 10.1104/pp.102.4.1193.
- Morkunas I, Ratajczak L (2014). The role of sugar signaling in plant defense responses against fungal pathogens. *Acta Physiologicae Plantarum* **36**: 1607–1619. DOI 10.1007/s11738-014-1559-z.

- Morkunas I, Bednarski W (2008). *Fusarium oxysporum* induced oxidative stress and antioxidative defenses of yellow lupin embryo axes with different levels of sugars. *Journal of Plant Physiology* **165**: 262–277. DOI 10.1016/j.jplph.2007.01.020.
- Ning Y, Wang Y, Fang Z, Zhuang M, Zhang Y, Lv H, Liu Y, Li Z, Yang L (2019). Comparative transcriptome analysis of cabbage (*Brassica oleracea* var. capitata) infected by *Plasmiodiophora brassicae* reveals drastic defense response at secondary infection stage. *Plant and Soil* **443**: 167–183. DOI 10.1007/s11104-019-04196-6.
- Olszak M, Truman W, Stefanowicz K, Sliwinska E, Ito M, Walerowski P, Rolfe S, Malinowski R (2019). Transcriptional profiling identifies critical steps of cell cycle reprogramming necessary for *Plasmiodiophora brassicae*-driven gall formation in *Arabidopsis*. *Plant Journal* **97**: 715–729. DOI 10.1111/tpj.14156.
- Prerostova S, Dobrev PI, Konradyova V, Knirsch V, Gaudinova A, Kramna B, Kazda J, Ludwig-Müller J, Vankova R (2018). Hormonal responses to *Plasmiodiophora brassicae* infection in *Brassica napus* cultivars differing in their pathogen resistance. *International Journal of Molecular Sciences* **19**: 4024. DOI 10.3390/ijms19124024.
- Raa J (1971). Indole-3-acetic acid levels and the role of indole-3-acetic acid oxidase in the normal root and club-root of cabbage. *Physiologia Plantarum* **25**: 130–134. DOI 10.1111/j.1399-3054.1971.tb01101.x.
- Raffaele S, Leger A, Roby D (2009). Very long chain fatty acid and lipid signaling in the response of plants to pathogens. *Plant Signaling & Behavior* **4**: 94–99. DOI 10.4161/psb.4.2.7580.
- Robin AHK, Hossain MR, Kim HT, Nou IS, Park JI (2019). Role of cytokinins in clubroot disease development. *Plant Breeding and Biotechnology* **7**: 73–82. DOI 10.9787/PBB.2019.7.2.73.
- Siemens J, Keller I, Sarx J, Kunz S, Schuller A, Nagel W, Schmülling T, Parniske M, Ludwig-Müller J (2006). Transcriptome analysis of *Arabidopsis* clubroots indicate a key role for cytokinins in disease development. *Molecular Plant-Microbe Interactions* **19**: 480–494. DOI 10.1094/MPMI-19-0480.
- Tenhaken R, Levine A, Brisson LF, Dixon RX, Lamb C (1995). Function of the oxidative burst in hypersensitive disease resistance. *Proceedings of the National Academy of Sciences of the United States of America* **92**: 4158–4163. DOI 10.1073/pnas.92.10.4158.
- Thomma BP, Eggermont K, Penninckx IA, Mauch-Mani B, Vogelsang R, Cammue BP, Broekaert WF (1998). Separate jasmonate-dependent and salicylate-dependent defense-response pathways in *Arabidopsis* are essential for resistance to distinct microbial pathogens. *Proceedings of the National Academy of Sciences of the United States of America* **95**: 15107–15111. DOI 10.1073/pnas.95.25.15107.
- Wagner G, Charton S, Lariagon C, Laperche A, Lugan R, Hopkins J, Frenco P, Bouchereau A, Delourme R, Gravot A, Manzanares-Dauleux MJ (2012). Metabotyping: A new approach to investigate rapeseed (*Brassica napus* L.) genetic diversity in the metabolic response to clubroot infection. *Molecular Plant-Microbe Interactions* **25**: 1478–1491. DOI 10.1094/MPMI-02-12-0032-R.
- Williams PH (1966). A system for the determination of races of *Plasmiodiophora brassicae* that infect cabbage and rutabaga. *Phytopathology* **56**: 624–626.
- Xiao HM, Cai WJ, Ye TT, Ding J, Feng YQ (2018). Spatio-temporal profiling of abscisic acid, indoleacetic acid and jasmonic acid in single rice seed during seed germination. *Analytica Chimica Acta* **1031**: 119–127. DOI 10.1016/j.aca.2018.05.055.
- Yahaya N, Petriacq P, Burrell M, Walker H, Malinowski R, Rolfe S (2017). Changes of metabolites status in plant pathogen interaction. *Advanced Science Letters* **23**: 4623–4626. DOI 10.1166/asl.2017.8947.
- Yan X, Chen S (2007). Regulation of plant glucosinolate metabolism. *Planta* **226**: 1343–1352. DOI 10.1007/s00425-007-0627-7.
- Zeier J (2013). New insights into the regulation of plant immunity by amino acid metabolic pathways. *Plant, Cell & Environment* **36**: 2085–2103. DOI 10.1111/pce.12122.
- Zhang X, Liu Y, Fang Z, Li Z, Yang L, Zhuang M, Zhang Y, Lv H (2016). Comparative transcriptome analysis between broccoli (*Brassica oleracea* var. italica) and wild cabbage (*Brassica macrocarpa* Guss.) in response to *Plasmiodiophora brassicae* during different infection stages. *Frontiers in Plant Science* **7**: 1929. DOI 10.3389/fpls.2016.01929.
- Zhu G, Ou Q, Zhang T, Jiang X, Sun G, Zhang N, Wang K, Fang H, Wang M, Sun J, Ge T (2013). A more desirable balanced polyunsaturated fatty acid composition achieved by heterologous expression of $\Delta 15/\Delta 4$ desaturases in mammalian cells. *PLoS One* **8**: e84871. DOI 10.1371/journal.pone.0084871.
- Zhu H, Zhai W, Li X, Zhu Y (2019). Two QTLs controlling Clubroot resistance identified from Bulk Segregant Sequencing in Pakchoi (*Brassica campestris* ssp. *chinensis* Makino). *Scientific Reports* **9**: 9228. DOI 10.1038/s41598-019-44724-z.

Supplementary Materials

Additional Figure 1. Galactose metabolism pathway showing differentially accumulated metabolites between *P. brassicae* infected susceptible (CM) and resistant (CCR) *B. rapa* genotypes. Red – significantly up-accumulated, green – significantly down-accumulated, and blue – detected but not significantly accumulated.

Additional Figure 2. Ascorbate and aldarate metabolism pathway showing differentially accumulated metabolites between *P. brassicae* infected susceptible (CM) and resistant (CCR) *B. rapa* genotypes. Red – significantly up-accumulated, green – significantly down-accumulated, and blue – detected but not significantly accumulated.

Additional Figure 3. Pentose and glucuronate interconversions pathway showing differentially accumulated metabolites between *P. brassicae* infected susceptible (CM) and resistant (CCR) *B. rapa* genotypes. Red – significantly up-accumulated, green – significantly down-accumulated, and blue – detected but not significantly accumulated.

Additional Figure 4. Riboflavin metabolism pathway showing differentially accumulated metabolites between *P. brassicae* infected susceptible (CM) and resistant (CCR) *B. rapa* genotypes. Red – significantly up-accumulated, green – significantly down-accumulated, and blue – detected but not significantly accumulated.

Additional Table 1. Differentially accumulated metabolites between susceptible *B. rapa* genotype - CM 28 days post infection with *P. brassicae* and control (CM-CK).

Additional Table 2. Differentially accumulated metabolites between resistant *B. rapa* genotype - CCR 28 days post infection with *P. brassicae* and control (CCR-CK).

Additional Table 3. Differentially accumulated metabolites between resistant - CCR and susceptible - CM *B. rapa* genotypes 28 days post infection with *P. brassicae*.

Additional Table 4. Differentially accumulated metabolites between controls (non-inoculated) of the resistant - CCR and susceptible - CM *B. rapa* genotypes.